Terahertz emission from $Bi_2Sr_2CaCu_2O_{8+\delta}$ intrinsic Josephson junction stacks with all-superconducting electrodes

2012 Supercond. Sci. Technol. 25 075015

(http://iopscience.iop.org/0953-2048/25/7/075015)

Supercond. Sci. Technol. **25** (2012) 075015 (5pp) doi:10.1088/0953-2048/25/7/075015

Terahertz emission from $Bi_2Sr_2CaCu_2O_{8+\delta}$ intrinsic Josephson junction stacks with all-superconducting electrodes

J Yuan[1], M Y Li[1,2], J Li[1,3], B Gross[4], A Ishii[1], K Yamaura[1,3], T Hatano[1], K Hirata[1], E Takayama-Muromachi[1,3], P H Wu[2], D Koelle[4], R Kleiner[4] and H B Wang[1,2]

[1] National Institute for Materials Science, Tsukuba 3050047, Japan
[2] Nanjing University, Nanjing 210093, People's Republic of China
[3] Hokkaido University, Sapporo, Hokkaido 060-0810, Japan
[4] Physikalisches Institut and Center for Collective Quantum Phenomena in LISA$^+$ Universität Tübingen, Auf der Morgenstelle 14, D-72076 Tübingen, Germany

E-mail: Kleiner@uni-tuebingen.de and WANG.Huabing@nims.go.jp

Received 8 February 2012, in final form 2 May 2012
Published 15 June 2012
Online at stacks.iop.org/SUST/25/075015

Abstract
Terahertz (THz) emission has been recently detected from intrinsic Josephson junction (IJJ) stacks made of the high critical temperature superconductor $Bi_2Sr_2CaCu_2O_{8+\delta}$ (BSCCO). The most employed structure is a mesa standing on a big pedestal of a single crystal with a thin gold layer as its top electrode. In this work, a large ($300 \times 50 \times 1.2\ \mu m^3$) IJJ stack with superconducting electrodes was fabricated and studied. The stack consisted of $N \approx 800$ IJJs. It was prepared with a double-sided fabrication process, and significant THz emission was detected. The output power is comparable to the emission power detected from mesa structures, obviously not weakened by the superconducting upper electrode. The observation of THz emission from the double-sided structure suggests that off-chip THz emission from IJJs can be obtained not only from mesa structures and, most importantly, that the emission power can be potentially enhanced in integrated multi-stack radiation sources.

(Some figures may appear in colour only in the online journal)

1. Introduction

Terahertz (THz) technology has attracted increasing attention for a wide range of applications in detecting and imaging, such as high-altitude telecommunications, public security, food quality control and environmental monitoring [1, 2]. Although many techniques like femtosecond laser pulses, quantum cascade lasers, synchrotron light, backward wave oscillators, etc, have been introduced to generate THz electromagnetic waves, their high cost and complexity limits applications. The lack of cost-effective and active devices results in the 'THz gap' problem [3]. According to the theory of the ac Josephson effect, a Josephson junction can work as a dc-voltage to high-frequency current converter, with 1 mV corresponding to 483 GHz. This provides the basis of superconducting high-frequency detectors and tunable radiation sources. However, the radiation frequency f of Josephson junctions is limited by the superconducting energy gap, which restricts the operation of conventional junctions down to 700 GHz or less. Moreover, the low output power, in the picowatt to nanowatt range, limits the applicability of a single junction. Intrinsic Josephson junctions (IJJs) in BSCCO [4] can overcome both problems. They can be operated at THz frequencies and stacking of many IJJs is possible. Recently, coherent off-chip THz radiation with an extrapolated output power of some microwatt was observed from stacks (mesa structures) of more than 600 IJJs with lateral dimensions in the 100 μm range [5]. For comparison, the Josephson length $\lambda_J \approx 0.5$ μm. It was assumed that the mesa forms an electromagnetic cavity and the Josephson oscillations in the individual junctions are synchronized by the alternating electromagnetic field stored in the cavity resonance. This finding triggered numerous experimental [6–16] and theoretical [17–35] studies to understand the mechanism of emission and to improve the performance of the radiation source.

Since there is no applicable single stack emitter, it is naturally expected to increase the output power by integrating several stacks into one device. If this is done with mesa structures one faces several problems: (1) mesas are typically contacted by normal conducting Au leads, leading to a finite contact resistance and additional power dissipation [36, 37]; (2) the mesa surface is often degraded, leading to surface junctions with a strongly reduced critical current density [37, 38]; (3) due to the mesa etching process the mesas have a trapezoidal cross-section, leading to a gradient in the critical currents of the IJJs [8]. These properties make it hard to achieve complete synchronization within a stack. Synchronization is even harder between different stacks. In our previous work, a double-sided fabrication process was applied in the preparation of small ($\sim$10 μm^2) IJJ stacks consisting of some ten junctions, as well as junction stack arrays [39, 40]. In this work well-controlled uniformity in both lateral dimension and junction number was demonstrated. We adopt this technique now to fabricate large IJJ stacks. The development of large stacks in a double-sided structure is a promising way to integrate radiation sources and perhaps also to address the issue of the mechanism of THz emission.

2. Experimental details

In the present experiment, the single crystals were grown by a floating zone technique in a four-lamp arc imaging furnace. They were annealed in a temperature range of 600–650 °C in an Ar 99%, O_2 1% atmosphere for 48–72 h. The crystals were slightly underdoped with a superconducting transition temperature (T_c) of 83–87 K.

The double-sided fabrication process for small IJJ stacks is described in detail in [39]. Here we outline some critical steps, shown in figure 1, to emphasize the modifications required to produce large stacks.

First, the ($\approx$50 μm thick) BSCCO single crystals were glued on a Si substrate with epoxy. A 30–40 nm thick Au thin film was deposited soon after the final cleaving step. A 600 $\times$ 600 μm^2 large square was patterned on the upper surface and etched by ion milling, leaving a mesa (about 2.0 μm thick) sitting on the BSCCO pedestal. A slit, 10 μm wide and 1.5 μm deep, was fabricated through the square mesa with its direction parallel with one boundary; two mesa-like structures sitting on top of the original square are formed during this step (see figure 1(a)). Then, the patterned single crystal surface was glued onto a MgO substrate and turned upside-down. The Si substrate was removed together with most of the BSCCO pedestal and the remnant pedestal was removed by an adhesive tape. Then a 30–40 nm thick Au thin

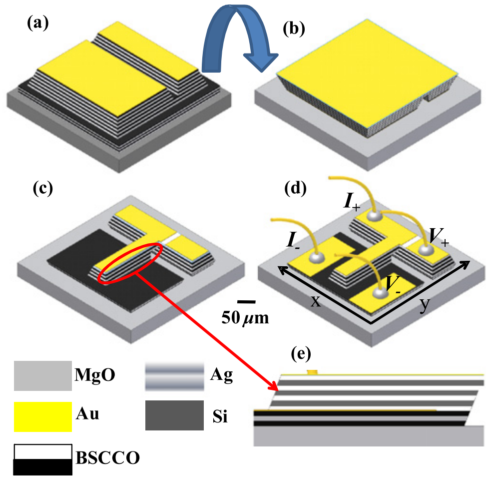

Figure 1. (a)–(d) A schematic diagram of the critical steps in the fabrication process. I_+, I_-, V_+ and V_- in (d) indicate current and voltage leads. (e) View parallel to the short side of the stack showing that the cross-section parallel to the long side of the stack approximates a parallelogram.

film was evaporated on this freshly cleaved surface. The link between the two mesas underneath is about 0.5 μm thick (see figure 1(b)). Next, a T shaped structure was patterned on this surface, with its cross bar located above one of the mesas created by the slit. The stem of the T crosses the slit and is mainly located on top of the other mesa. After ion milling the cross bar forms the bank contacting the upper surface of the IJJ stack. The stack itself is formed by the lower part of the stem (see figure 1(c)). Finally, four gold electrodes were made for current–voltage (I–V) measurements. The electrodes were connected to gold wires by silver paste, as shown in figure 1(d). The final structure contains an IJJ stack about 300 $\times$ 50 μm^2 in size, as sketched in figure 1(d). Its thickness is about 1.2 μm, corresponding to a stack of $\approx$800 IJJs, and it is connected to the ($\approx$0.3 μm thick) leads by BSCCO layers. Note that, because in this double-sided fabrication process Ar ion beams of opposite direction are used to etch different walls of the stack (the sample does not rotate during ion milling), its cross-section parallel to the long side forms a parallelogram rather than a trapezoid, see figure 1(e). The cross-section parallel to the short side is still trapezoidal. The angle between the Ar ion beam and the mesa surface is 45°, and the beam is along the long side of the stack. Under this condition, the steepness of the long-side wall of the stack (about 45°, as checked by atomic force microscopy (AFM)) is steeper than that obtained by a vertical beam (it is about 35° for our process). Overall, the junction areas become more uniform.

The samples were mounted in a continuous He flow cryostat. A four-terminal method was employed in the I–V measurement, as indicated in figure 1(d). In order to have stable operation, the junctions were biased using a current source driven by batteries. Emission data and frequency spectra were measured in a self-made interferometer using a Si bolometer for THz detection (see figure 2). The direction of detection is perpendicular to the BSCCO *ab* planes. The

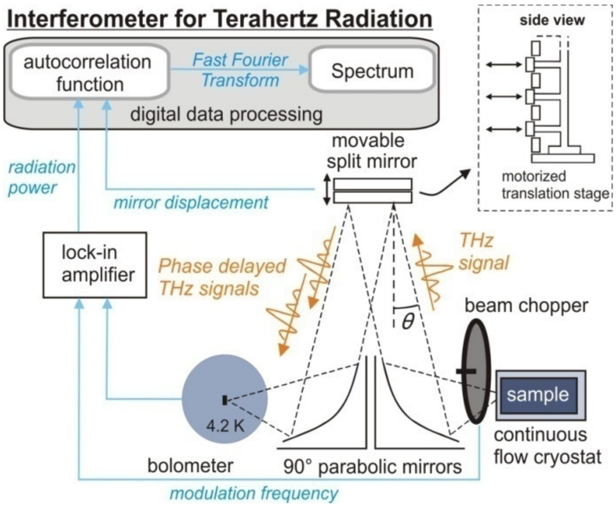

Figure 2. Schematic diagram of the experimental setup for THz detection.

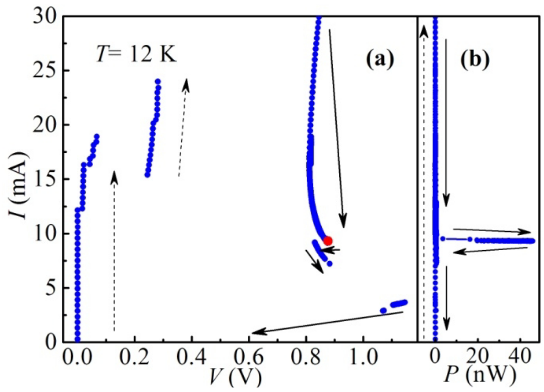

Figure 3. Experimental data with a double-sided IJJ stack at $T = 12$ K. (a) dc current–voltage curve; (b) emission power detected by bolometer versus current through the stack. Arrows indicate the direction of the current sweep. The red point in (a) indicates the bias point where the largest emission was detected.

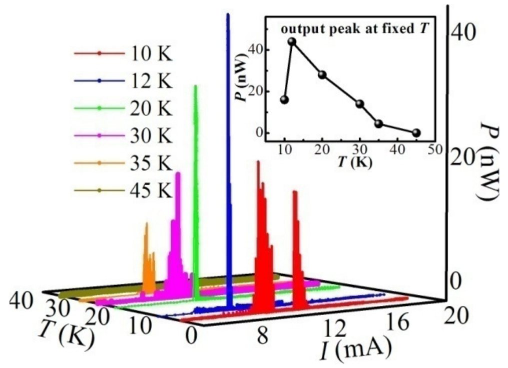

Figure 4. THz emission power versus bias current at various temperatures. The inset shows the temperature dependence of the emission peak with maximal output power.

light path from the emitter to the Si bolometer is about 1 m. The solid angle of our setup, defined by the aperture of the Winston cone in front of the bolometer, is 0.04 solid radians. The THz emission power from the double-sided stack was detected during the I–V scans and recorded simultaneously. Numbers for the emission power given below refer to the power detected by the bolometer. The frequency spectrum was obtained with the junctions being biased at fixed current. The details of the setup have been described elsewhere [10].

3. Results and discussion

Figure 3(a) shows an I–V curve of the double-sided sample at 12 K. Increasing I from zero one finds various jumps to resistive branches until, at $I \approx 25$ mA, the whole stack switches to the resistive state. When decreasing I in this fully resistive state one finds a region of negative differential resistance, very similar to the case of conventional mesa structures. Note that since the stack is connected with two superconducting electrodes, there is no contact resistance or strongly degraded surface junctions involved in the I–V measurements. We still observe some branches where switching occurs at reduced bias current, but the effect is much less pronounced than in mesa structures.

Figure 3(b) shows the detected THz signal versus I. A strong signal was observed in the fully resistive state of the stack at $I = 9.3$ mA, i.e. in the back-bending region of the I–V curves. The maximum detected emission power is about 45 nW, comparable to the emission power obtained from conventional mesa structures. At least for mesas the emission power is strongly angle dependent, with a maximum near 30° away from the c-axis [11, 15]. For simplicity, ignoring this angle dependence and integrating over the half-space above the substrate plane we find an integrated power of roughly 5 μW.

Figure 4 shows the current dependence of the detected emission power at various temperatures. The THz emission signal appeared in the fully resistive state and was observed in the temperature range from 10 to 45 K. Depending on temperature one or more emission peaks appeared. The largest one is at $T = 12$ K, i.e. close to the lower boundary of the temperature region where THz emission can be detected.

As to the emission frequency at the main output peak, the performance of the emitter is shown in figure 5. At the maximum radiation points, the voltage across the stack and emission signals are stable, allowing for measurements of the frequency spectrum by the interferometer. Graph (a) shows the spectrum at $T = 12$ K, $I = 9.3$ mA, and $V = 0.877$ V, where the maximum emission power was detected. The peak frequency is $f_p = 0.53$ THz, with a linewidth of 10 GHz, which is limited by the resolution of our setup (also at other temperatures the detected linewidths were resolution limited). According to the Josephson relation $V/N = \Phi_0 f$, we can calculate the junction number $N = 794$, close to the value estimated from the fabrication process. Graph (b) shows N versus T for various temperatures between 10 and 45 K. For temperatures of 12, 20 and 45 K, N is close to the value of 800 expected from the thickness of the stack. At $T =$ 10 K N is slightly higher but within the error bars. At $T = 30$ and 35 K we seem to have lost some junctions. Graph (c) shows f_p versus T. The frequency interval where emission was

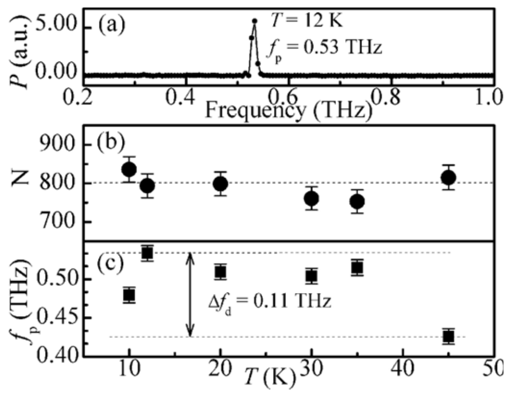

Figure 5. (a) Frequency spectrum of the detected emission at $T = 12$ K, $I = 9.3$ mA and $V = 0.877$ V, compare with figure 3(a). (b) Junction number (N) versus temperature. The dashed line indicates $N = 800$ expected from the thickness of the stack. (c) Peak frequency versus temperature.

observable is $\Delta f_d = 0.11$ THz. Note that the lowest values of f_p occur at, respectively the lowest and highest temperatures. The reason for this is unclear to us.

The observed maximum emission power is comparable to the emission power obtained from conventional mesa structures [5, 10, 11]. It was reported that a thick top upper electrode would hinder THz radiation from an IJJ stack [41]. This apparently is not the case, a finding which may trigger further understanding in the mechanism of generating coherent THz radiation from BSCCO IJJ stacks.

In the data shown above, the largest emission signals have been detected at high bias current. In fact, here the electrothermal behavior is different from that at low bias, where there is only little overheating of the stack. In the high bias regime, Joule heating leads to a non-homogeneous temperature distribution in the stack which may be well above the bath temperature in certain parts. As has been shown for mesa structures, above a certain current a hotspot (a region heated to a temperature above T_c) can form, typically near the point of current injection [6, 9, 10, 31, 41]. The position and size of the hotspot varies as the bias current changes, which will adjust some physical parameters in the stack. For instance, the hotspot can vary the resonance frequency of the cavity by changing the mode velocity and the size of the cold part of the mesa. In this way, the efficiency of synchronization from the cavity can be tuned by the hot spot. Often—although not always—the strongest emission is observed in this hotspot regime. As will be discussed elsewhere [42], a hotspot also appears in the double-sided structures. Here, heating is determined by the intrinsic properties of the single crystal itself, rather than being influenced by normal conducting contacts to the IJJ stack. As a consequence, the hotspot formation is very reproducible for stacks of a given geometry, a property which we believe is relevant for controlled THz emission. Further, as already mentioned, in the conventional fabrication process the shape of the mesa structure is usually a trapezoidal platform. The nonuniformity in junction area is a problem for synchronizing a large number of junctions [13]. In the double-sided fabrication process the nonuniformity in junction area is reduced, since two sides of the stack form a parallelogram, as shown in figure 1. This might help to fabricate more uniform, thick IJJ stacks for a powerful emitter.

However, the main advantage of the double-sided fabrication process is that various superconducting elements can be integrated in an all-superconducting structure. From the schematic diagram of figure 1 one can see that the electrodes on the other bank of the slit can be patterned into various elements such as antennas, additional stacks or other structures. It has been shown previously that arrays of stacks with superconducting interconnections, middle electrodes to a stack, antennas, or other integrated circuits can be realized from a single BSCCO crystal [39, 40, 43, 44]. This should have advantages compared to structures where different elements are connected by normal metal wires, e.g. by reducing resistive losses.

4. Conclusions

To conclude, we have successfully fabricated large size double-sided BSCCO IJJ stacks. In this way, the junction number in the stack can be well controlled and superconducting leads to the stack can be made. THz radiation comparable in power and frequency to conventional mesa structures was obtained. It seems that these double-sided IJJ THz emitter structures are helpful in making integrated radiation sources based on intrinsic Josephson junctions in high T_c superconductors. The result that THz emission from BSCCO stacks is not weakened by a thick superconducting upper electrode possibly triggers further understanding of THz emitters in IJJ stacks.

Acknowledgments

Financial support by the strategic Japanese–German International Cooperative Program of the JST and the DFG, and by Grants-in-Aid for scientific research from JSPS is gratefully acknowledged.

References

[1] Tonouchi M 2007 *Nature Photon.* **1** 97
[2] Lee M and Wanke M C 2007 *Science* **316** 64
[3] Ferguson B and Zhang X C 2002 *Nature Mater.* **1** 26
[4] Kleiner R, Steinmeyer F, Kunkel G and Muller P 1992 *Phys. Rev. Lett.* **68** 2394
[5] Ozyuzer L *et al* 2007 *Science* **318** 1291
[6] Wang H B, Guénon S, Yuan J, Iishi A, Arisawa S, Hatano T, Yamashita T, Koelle D and Kleiner R 2009 *Phys. Rev. Lett.* **102** 017006
[7] Minami H, Kakeya I, Yamaguchi H, Yamamoto T and Kadowaki K 2009 *Appl. Phys. Lett.* **95** 232511
[8] Ozyuzer L *et al* 2009 *Supercond. Sci. Technol.* **22** 114009
[9] Guénon S *et al* 2010 *Phys. Rev.* B **82** 214506
[10] Wang H B *et al* 2010 *Phys. Rev. Lett.* **105** 057002
[11] Tsujimoto M, Yamaki K, Deguchi K, Yamamoto T, Kashiwagi T, Minami H, Tachiki M, Kadowaki K and Klemm R A 2010 *Phys. Rev. Lett.* **105** 037005
[12] Koseoglu H, Turkoglu F, Simsek Y and Ozyuzer L 2011 *J. Supercond. Novel Magn.* **24** 1083–6

[13] Benseman T M, Koshelev A E, Gray K E, Kwok W K, Welp U, Kadowaki K, Tachiki M and Yamamoto T 2011 *Phys. Rev.* B **84** 064523
[14] Yamaki K, Tsujimoto M, Yamamoto T, Furukawa A, Kashiwagi T, Minami H and Kadowaki K 2011 *Opt. Express* **19** 3193
[15] Kashiwagi T *et al* 2012 *Japan. J. Appl. Phys.* **51** 010113
[16] Tsujimoto M *et al* 2012 *Phys. Rev. Lett.* **108** 107006
[17] Bulaevskii L N and Koshelev A E 2007 *Phys. Rev. Lett.* **99** 057002
[18] Koshelev A E 2008 *Phys. Rev.* B **78** 174509
[19] Lin S Z and Hu X 2008 *Phys. Rev. Lett.* **100** 247006
[20] Krasnov V M 2009 *Phys. Rev. Lett.* **103** 227002
[21] Klemm R A and Kadowaki K 2010 *J. Phys.: Condens. Matter* **22** 37
Klemm R A and Kadowaki K 2010 *J. Supercond. Novel Magn.* **23** 613
[22] Nonomura Y 2009 *Phys. Rev.* B **80** 140506
[23] Tachiki M, Fukuya S and Koyama T 2009 *Phys. Rev. Lett.* **102** 127002
[24] Koyama T, Matsumoto H, Machida M and Kadowaki K 2009 *Phys. Rev.* B **79** 104522
[25] Pedersen N F and Madsen S 2009 *IEEE Trans. Appl. Supercond.* **19** 726–9
[26] Savel'ev S, Yampol'skii V A, Rakhmanov A L and Nori F 2010 *Rep. Prog. Phys.* **73** 026501
[27] Hu X and Lin S Z 2010 *Supercond. Sci. Technol.* **23** 053001
[28] Zhou W, Wang C and Chen Q H 2010 *Phys. Rev.* B **82** 184514
[29] Koshelev A E 2010 *Phys. Rev.* B **82** 174512
[30] Tachiki M, Ivanovic K and Kadowaki K 2011 *Phys. Rev.* B **83** 014508
[31] Yurgens A 2011 *Phys. Rev.* B **83** 184502
[32] Lin S Z, Hu X and Bulaevskii L 2011 *Phys. Rev.* B **84** 104501
[33] Slipchenko T M, Kadygrob D V, Bogdanis D, Yampol'skii V A and Krokhin A A 2011 *Phys. Rev.* B **84** 224512
[34] Krasnov V M 2011 *Phys. Rev.* B **83** 174517
[35] Asai H, Tachiki M and Kadowaki K 2012 *Phys. Rev.* B **85** 064521
[36] Doh Y J, Lee H J and Chang H S 2000 *Phys. Rev.* B **61** 3620
[37] Doh Y J, Kim J H, Kim K T and Lee H J 2000 *Phys. Rev.* B **61** R3834
[38] Li S X, Qiu W, Han S, Wei Y F, Zhu X B, Gu C Z, Zhao S P and Wang H B 2007 *Phys. Rev. Lett.* **99** 037002
[39] Wang H B, Wu P H, Chen J, Maeda K and Yamashita T 2002 *Appl. Phys. Lett.* **80** 1604
[40] Wang H B, Wu P H and Yamashita T 2001 *Appl. Phys. Lett.* **78** 4010
[41] Kakeya I, Omukai Y, Yamamoto T, Kadowaki K and Suzuki M 2011 *Superconducting Centennial Conf. (Den Haag, Sept. 2011)*
[42] Gross B *et al* 2012 unpublished
[43] Wang H B, Hatano T, Yamashita T, Wu P H and Muller P 2005 *Appl. Phys. Lett.* **86** 023504
[44] Wang H B, Chen J, Wu P H, Yamashita T, Vasyukov D and Müller P 2003 *Supercond. Sci. Technol.* **16** 1375